Chapter 55

Probing the Interiors of Planets with Geophysical Tools

W. Bruce Banerdt
Jet Propulsion Laboratory, California Institute of Technology, Pasadena, CA, USA

Véronique Dehant
Royal Observatory of Belgium, Brussels, Belgium

Robert Grimm
Southwest Research Institute, Boulder, CO, USA

Matthias Grott
German Aerospace Center (DLR), Institute of Planetary Research, Berlin, Germany

Philippe Lognonné
Institut de Physique du Globe de Paris, Paris, France

Suzanne E. Smrekar
Jet Propulsion Laboratory, California Institute of Technology, Pasadena, CA, USA

Chapter Outline

1. Introduction **1185**
2. Investigating Planetary Interiors Using Seismology **1186**
2.1. Terrestrial Seismology 1186
2.2. Lunar Seismology 1187
2.3. Mars Seismology 1190
2.4. Jovian Seismology 1190
3. Investigating Planetary Interiors Using Gravity and Dynamics **1190**
4. Investigating Planetary Interiors Using Heat Flow Measurements **1192**
4.1. Measurement Techniques 1192
4.2. The Heat Flow of the Earth 1193
4.3. Lunar Heat Flow 1194
4.4. Future Investigations 1196
5. Investigating Planetary Interiors Using EM Sounding **1198**
5.1. Natural Sources 1198
5.2. Measurement Techniques 1199
5.3. Terrestrial Exploration 1199
5.4. Magnetic Sounding of the Moon 1200
5.5. Magnetic Sounding of the Galilean Satellites 1201
5.6. Future Exploration 1202
6. Summary **1203**
Bibliography **1203**

1. INTRODUCTION

Understanding the structure and processes of the deep interior of the planets is crucial for understanding their origin and evolution, as well as the surface history and processes. Planetary interiors record evidence of conditions of planetary **accretion** and **differentiation**. The crust of a planet is generally thought to form initially through **fractionation** of an early magma ocean, with later addition through partial melting of the mantle and resulting volcanism. Thus the volume (thickness) and structure of the crust can place strong constraints on the depth and evolution of a putative magma ocean. Interior processes also exert significant control on surface environments. The structure of a planetary interior and its dynamics control heat transfer within a planet through **advected** mantle material, heat conducted through the lithosphere, and volcanism.

Encyclopedia of the Solar System. http://dx.doi.org/10.1016/B978-0-12-415845-0.00055-4
2014 Published by Elsevier Inc.

Volcanism in particular controls the timing of volatile release, and influences the availability of water and carbon. The existence and strength of any planetary magnetic field depends in part on the size and state of the core.

Even the comprehension of how life developed and evolved on the Earth requires knowledge of the Earth's thermal and volatile evolution and how mantle and crustal heat transfer, coupled with volatile release, affected habitability at and near the planet's surface. Although geophysics can provide information about past processes and states required to reach this understanding, it primarily provides a "snapshot" at the present time of how the Earth behaves. This "boundary condition" is a powerful constraint on all models that describe the history of the Earth and attempt to place the evolution of life in this framework, as such models must evolve to this present state.

However, this realm of the deep planetary interior is inaccessible to direct observation, with tens to thousands of kilometers of rock blocking our "view"; note that the deepest hole ever drilled is the Kola SG-3 in Russia, which reached 12.262 km in 1989. Whereas some deep material is inevitably transported to the surface (for example, through volcanism, impact excavation, and outgassing), these materials typically undergo complex changes on their journey that are difficult to unravel and are subject to sampling biases, and thus provide limited insight.

The most effective way to explore the interior of a planet is through geophysics, as it provides tools that allow for "remote sensing" of the interior. Seismology, together with surface heat flow, magnetic and gravity field measurements, and electromagnetic (EM) techniques, have revealed the basic internal workings of the Earth: its thermal structure, its compositional **stratification**, as well as significant lateral variations in these quantities. For example, seismological, magnetic, and **paleomagnetic** measurements revealed the basic components of seafloor spreading and subduction, and seismology and EM measurements have mapped the structure of the core, compositional and phase changes in the mantle, three-dimensional velocity anomalies in the mantle related to **subsolidus convection**, and lateral variations in lithospheric structure. Additionally, seismic information placed strong constraints on Earth's interior temperature distribution and the mechanisms of **geodynamo** operation (see Magnetic Field Generation).

This chapter describes the four major classes of geophysical techniques that are used to probe deep planetary interiors: seismology, geodesy (which includes both gravimetry and planetary dynamics), heat flow, and electromagnetism. We choose to exclude techniques that have limited penetration depths (such as gamma-ray scattering, which samples to about a meter; microwave/radar techniques, which penetrate a few meters to a few kilometers; and active/exploration seismology, which typically concerns itself with depths less than 10 km), as well as a few exotic techniques (such as neutrino and muon tomography) whose use in planetary exploration is likely beyond any practical horizon.

2. INVESTIGATING PLANETARY INTERIORS USING SEISMOLOGY

2.1. Terrestrial Seismology

Seismology is the most powerful tool available for probing the interior of planets. Seismic waves (for terrestrial planets) or acoustic waves (for giant gas planets or the Sun) propagate at **seismic velocities**, or the speed of sound. These velocities, as well as the amplitude, polarization, and propagation direction of seismic waves, are directly related to quantities such as the temperature, pressure, and/or composition of the material through which the waves travel.

Modern seismology started in 1889, with the detection in Germany by Ernst von Rebeur-Paschwitz of ground displacements associated with waves generated by an earthquake in Japan. In quick succession, compositional (as manifested in seismic velocity) discontinuities between the mantle and core (the core–mantle boundary, or CMB, discovered by Richard Dixon Oldham in 1906) and the crust and mantle (the Moho discontinuity, discovered by Andrija Mohorovičić in 1909) were detected through the analysis of seismograms, as was the solid inner core, somewhat later, by Inge Lehmann in 1936 (Figure 55.1).

Waves are either reflected or **refracted** by these discontinuities, and they propagate in ways very similar to optical rays. Two types of **body waves** can propagate inside a planet: compressional waves (or P-waves), which generate pressure changes and displacements along the propagation direction, and shear waves (or S-waves), which do not generate a pressure change but rather displacements perpendicular to the propagation direction. The latter cannot exist in fluids and have velocities about 1.7 times smaller than the P velocities, and thus arrive after the P-waves. S-waves are fully reflected by solid–fluid boundaries, and these reflections are key to detecting underground fluids, such as the liquid iron of the outer core or underground oil and natural gas reservoirs. Because of its power and flexibility, seismology has been used extensively for both basic research and resource exploration, and now enables three-dimensional imaging of deep crustal structure or of the convection patterns in the Earth's mantle, through the small changes in seismic velocities generated by both temperature differences and the preferred orientation of the component crystals in mantle rocks in the direction of convective motion.

In addition to the crust–mantle and core–mantle boundaries, several additional global discontinuities have been found in the mantle and in the core by seismology. In the mantle, these discontinuities mark the transition between an olivine upper mantle (at 600 km depth for one

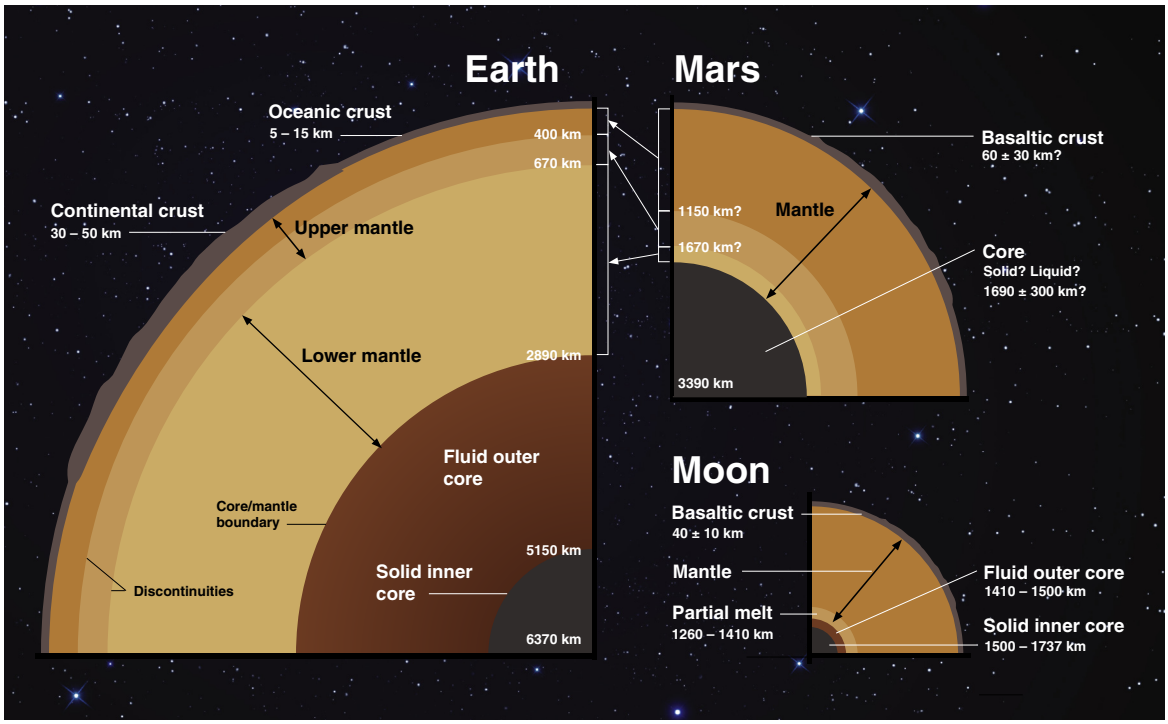

FIGURE 55.1 Interior structure of the Earth and Moon, as seen by seismology. The expected structure of Mars is shown in comparison. Shown are the depths to the major interior boundaries of the planets, between the crust, mantle, outer core, and inner core, as well as discontinuities at the two major phase boundaries. On the Moon there also appears to be a partially-molten zone at the base of the mantle. For the Earth the range of observed crust thicknesses are given, whereas for the Moon and Mars the uncertainty in the average crust thickness is shown. A smaller planet with weaker gravity has a slower pressure increase with depth; consequently, most of the Martian mantle is in a pressure state similar to the Earth's upper mantle, while most of the Moon's mantle corresponds to the conditions in only the first 300 km of the Earth.

of the most widely accepted average Earth models, called PREM, or Preliminary Reference Earth Model) and a perovskite lower mantle (at 770 km depth). In the region between these two discontinuities, called the transition zone, the dominant mineral, olivine, is in a spinel crystal structure. These two discontinuities may play a major role in controlling the convection of the mantle and therefore its geodynamic evolution. Much of modern seismology focuses on the details of these discontinuities, such as their topography or the thin transition zones just above the CMB (perhaps associated with a post-perovskite phase in the mantle) and outer-inner core boundary (due to the accumulation of lighter elements in a slushy layer just above the solid inner core).

Two other major discoveries have marked terrestrial seismology. The first was the measurement of global oscillations of the Earth, which are bell-like global vibrations with discrete periods directly related to the Earth's structure and composition. This was first done following the 1960 9.5 magnitude earthquake in Chile, which remains the largest earthquake ever observed with seismometers. These data, along with those subsequently recorded for quakes with magnitudes larger than 7–7.5, have revealed not only the natural resonant frequencies of the Earth (called eigenfrequencies, with periods ranging between 52 min and about 1 min) but also a fine structure of these tones, mathematically comparable to the fine structure of atoms in quantum mechanics.

The second major discovery was made in the early twenty-first century. Much of the ground noise measured during the quiet periods (when no coherent seismic waves from quakes are noticeable) is in fact the superposition of seismic waves excited by ocean waves and atmospheric winds and turbulence. It was shown that analysis of these vibrations can be used to measure not only the seismic speeds between two locations but also very small time variations of these seismic speeds, associated, for example, with changes in the structure of volcanoes prior, during and after an eruption or in the crustal structure after an earthquake. These findings opened the area of time-dependent seismology, which aims to detect temporal changes in the Earth's structure.

2.2. Lunar Seismology

In a sense, the long-term goal of planetary seismology is to repeat this geophysical success story on other planets. Planetary seismology began almost at the same time as space exploration itself; one of the instruments carried by the Ranger 3 mission, launched toward the Moon on January

26, 1962, was a seismometer. This first attempt, as well as those of Rangers 4 and 5 (also launched in 1962), all failed, but the first Apollo mission, Apollo 11, successfully deployed the first planetary seismometer. This instrument was powered by solar panels and did not survive the end of the second lunar day. The next five Apollo missions, however, each had a long-lived nuclear-powered seismometer called a Passive Seismic Experiment (PSE; Figure 55.2), able to record both long-period and high-frequency ground displacements. With the exception of Apollo 13, they were all successfully installed and worked until 1977, forming a network of four stations. This regional network (stations 12 and 14 were only about 180 km apart and formed one corner of an approximately equilateral triangle, with stations 15 and 16 at the other corners, each about 1100 km away), was complemented by local seismic arrays at the Apollo 15, 16, and 17 sites for active seismic studies of the shallow lunar subsurface. A gravimeter, deployed at the Apollo 17 site, was also able to detect seismic waves with a much lower sensitivity than the Apollo PSE seismometers. These instruments remain the only seismometers operated on the Moon, and this is likely to remain the case until at least 2020, as none of the confirmed missions of this decade plan to deploy new seismometers on the Moon.

Due to their extraordinary sensitivity, the Apollo PSE instruments revolutionized our understanding of the lunar interior. Even more surprising is that their data are still being used today to perform original research, more than 35 years after they were turned off.

The principle of a seismometer is to detect the small vibrations of the ground associated with passing seismic waves. Although technology development since the 1960s has allowed higher and higher sensitivities, the fundamental design on which virtually all seismometers are based has remained the same for more than 120 years: a mass, called the proof mass, supported by a spring. When the ground (and the instrument which is fixed to it) moves, the inertia of the mass causes it to remain stationary, which is physically equivalent to a motion with respect to the frame of the instrument. The displacement or velocity of the mass is detected by a transducer. The Apollo seismometers were able to detect ground displacement with amplitudes of about 0.5 Å, which is of the order of the radius of a hydrogen atom. These measurements were performed simultaneously by a three-axis (vertical and two mutually perpendicular horizontal directions) long-period instrument, focused on periods around 2 s, and by a single-axis (vertical) short-period instrument, focused on vibrations with periods of around 0.125 s.

These instruments discovered a seismically active Moon and detected about 12,500 moonquakes during more than 7 years of operation. The Moon is still only weakly active compared to the Earth; all these events have very small magnitudes with respect to terrestrial standards, and the largest moonquake has a **moment magnitude** (M) of only about 4, as compared to $M \sim 9.5$ of the largest quake detected on the Earth (the 1960 Chile earthquake). This is a factor of 10^8 smaller in terms of long-period amplitudes.

Three types of seismic signals were detected (Figure 55.3): about 30 were tectonic quakes, including the largest ones. Like most earthquakes, they occurred in the upper part of the planet, at depths no greater than about 200 km. Much more numerous (almost 9000 events) were the deep moonquakes, occurring at depths between 800 and 1200 km. These events were found to occur with the periodicity of the lunar orbit around the Earth, and occurred at a limited number of epicenters (less than 300), where quakes repeated regularly during the 7 years of network operations. These quakes appear to be associated with the solid-body tidal stresses caused by the Earth on the Moon, which are modulated by small variations of distance between the two bodies. Most of these quakes are very small, most with M smaller than 2 and only a few reaching magnitude 3. The last class of events is meteoroid impacts, with almost 2000 impacts detected. In contrast to the Earth, no atmosphere

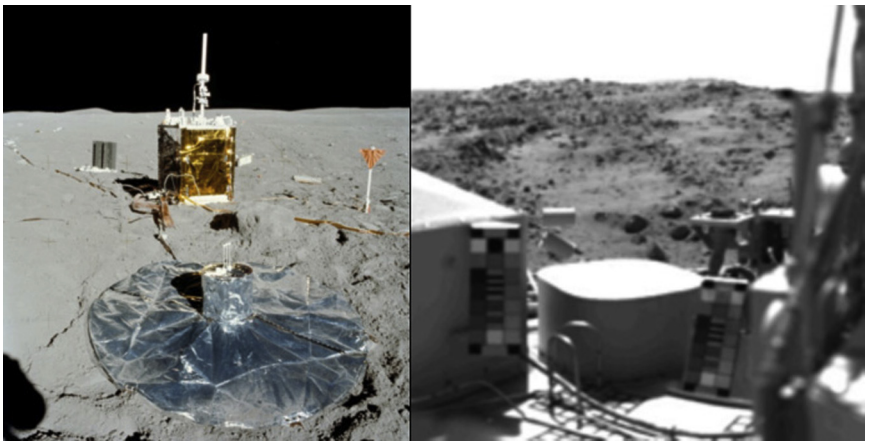

FIGURE 55.2 On the left is an Apollo PSE seismometer on the lunar surface. The image on the right shows the Viking seismometer, on the deck of the Viking Lander (the shorter box near the center of the picture).

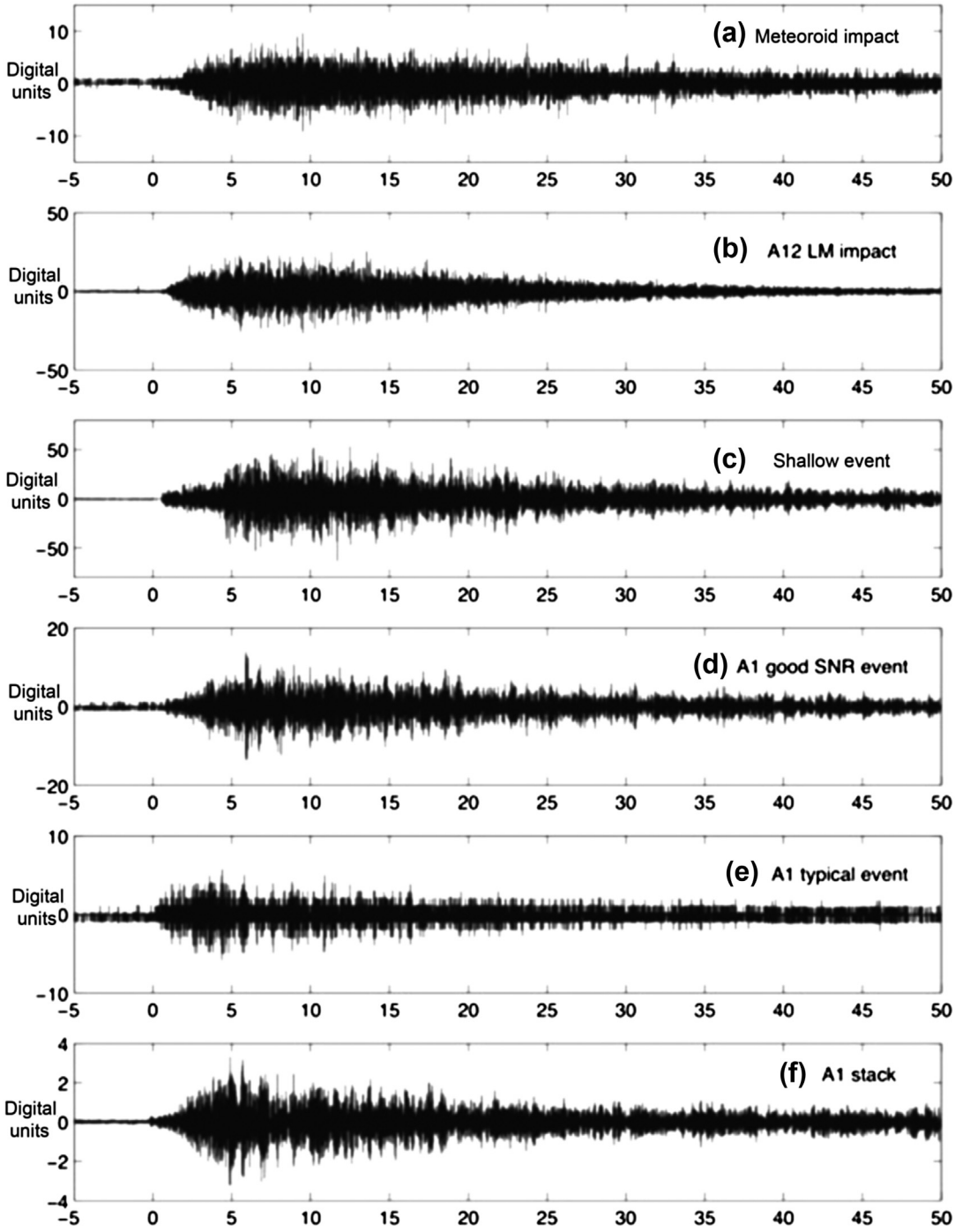

FIGURE 55.3 Examples of lunar seismograms for (a) natural impacts, (b) artificial impacts, (c) tectonic quakes, and (d–f) deep moonquakes. All seismograms are recorded on long period channels by the Apollo Passive Seismic Experiment; one digital unit corresponds to 0.5 Å of ground displacement at 0.5 Hz; *x*-axis is time in minutes. The tectonic quake in this example is one of the largest magnitude shallow events and has a comparable amplitude to the chosen artificial impact. Note the low amplitude and poor data quality of typical deep moonquakes in (e). However, the repeated similar waveforms of deep moonquakes from distinct source regions allows stacking of many events to improve the signal-to-noise ratio (f). Note: LM is Lunar Module, SNR is Signal-to-Noise Ratio. *From Lognonne and Johnson (2007).*

protects the Moon from **meteoroids**, and they can therefore generate seismic waves when they hit the lunar surface with mean impact velocities of about 20 km/s. All these seismic events were characterized with seismograms very different from those typically seen on the Earth. Due to the lack of atmosphere, the surface and subsurface lunar materials are extremely dry. Moreover, the billions of years of impacts have generated a highly fractured, low-seismic-velocity zone near

the lunar surface, which is very effective in trapping and scattering waves. These conditions result in extremely long duration (sometimes hours in length) seismic signals, even for very small quakes. Such long reverberations are never observed on the Earth.

Thanks to these seismic sources, both the location of many of these events and the associated travel time of the seismic waves between the **epicenter** and the seismic stations have been determined, enabling scientists to model the interior of the Moon and to identify a crust, a mantle, and a core, like on the Earth. The crustal thickness has a mean value of 40 ± 5 km. From there down to about 1400 km, a relatively homogeneous mantle was seen, possibly relatively hot and **attenuating** at depths larger than 1100−1200 km. And finally, a 350-km-radius liquid core was discovered in early 2012, more than 40 years after the transmission of the Apollo data, thanks to new seismic processing techniques and to the capability of the modern computers to perform calculations beyond the reach of the 1970s' Apollo seismologists. Seismology has also been able, through the measurement of seismic velocities in the mantle, to constrain the temperature at the bottom of the mantle. Because of the different melting temperatures for iron and iron alloys, this suggests that the lunar core is composed of iron mixed with some light element rather than pure iron. Evidence for seismic discontinuities in the lunar mantle remains weak. A possible discontinuity at a depth of 500 km, proposed by the Apollo seismic experiment team, is still controversial, as it might in fact be related to the poor resolution of the Apollo network at this depth. Thus much more remains to be done on the Moon in terms of seismology, and several prospective projects plan to redeploy seismometers on our natural satellite.

2.3. Mars Seismology

The seismic exploration of Mars was the logical next step after the Moon, and this motivated the inclusion of seismometers in the payload of the two Viking landers, launched by National Aeronautical and Space Administration (NASA) to Mars in 1976 (Figure 55.2). Unfortunately, due to cost and technical limitations, the seismometers were about 10,000 times less sensitive than the Apollo seismometers and were mounted on the lander deck, not placed in direct contact with the ground. In addition, the seismometer on Viking 1 failed to uncage (the seismometers were locked, or "caged", during flight to avoid damage) due to a technical failure. The seismometer onboard Viking 2 lasted for 19 months on Mars, but due to operational limitations it accumulated only a little more than 3 months of usable data and did not detect any marsquakes. During the day, the data were dominated by wind-generated lander vibrations, while during the night, its quality was limited by the seismometer's poor sensitivity and coupling to the ground. Given the various limitations, this lack of marsquake detection remains compatible with a Mars activity comparable to that of the Earth away from tectonic plate boundaries (where most of the activity is located). Thus it is generally accepted that Mars likely has a level of seismic activity between this upper limit and that of the Moon. Constraining this level of activity will be the first goal of the Interior exploration using Seismic Investigations, Geodesy and Heat Transport (InSight) project, which is currently under development by NASA. This mission aims to deploy a seismometer on Mars in September 2016, together with other geophysical sensors (heat flow, geodetic, and magnetic measurements, in addition to some atmospheric sensors).

2.4. Jovian Seismology

Mars' seismic activity will therefore remain hidden for a few more years. But the next planet, Jupiter, has finally revealed its continuous vibration after almost 30 years of attempted observations. In this case, data are obviously not coming from seismometers, but from remote observation through telescopes on the Earth. The technique consists of measuring the vertical velocity of the Jovian optical surface with spectroscopic techniques originally developed for solar and stellar seismology. Thanks to a steady increase in sensitivity, the observations have finally detected continuous oscillations with an amplitude of about 0.5 m/s, putting Jupiter third on the list of the bodies of the solar system for which global oscillations have been detected (after the Earth and the Sun). It is likely that a significant improvement in these observations will be made in the next 5 years, and we can therefore reasonably expect that by the end of this decade, comparative seismology will be possible among three terrestrial bodies (Earth, Moon, and Mars) and between two fluid ones (the Sun and Jupiter).

3. INVESTIGATING PLANETARY INTERIORS USING GRAVITY AND DYNAMICS

Historically, the most common method for exploring planetary interiors has been through observed variations in their gravitational fields, orientation, and rotation, which can be collectively described as geodesy. The data can be obtained as a by-product of the communication and navigation systems of planetary probes flying by, in orbit around, or landed on the planets. Gravity and rotation provide information primarily on the distribution of mass within a planet, including density differences due to overall structure (crust, mantle, and core) and from processes such as volcanism and tectonic deformation.

The major disadvantage of these techniques is their inherent ambiguity. It can be shown mathematically (**Gauss' theorem**) that for any gravity field measured

outside a body, there are an infinite number of distinct mass distributions inside the body that could generate that field (a similar result holds for rotational dynamics). While this seems daunting, in practice, there is usually other information that can be used to constrain the possible (or likely) distributions. Thus, geodetic methods are most powerful when used in combination with other techniques.

Spatial variations in the gravity field of planetary bodies are obtained by monitoring the trajectory of passing or orbiting spacecraft. For example, if an orbiter passes over a buried body with higher density than its surroundings, it will experience a higher gravitational attraction than otherwise and will be pulled slightly downward in its orbit. This deviation is determined via Doppler (which gives velocity) and ranging (which gives distance) measurements on radio links between the Earth and the spacecraft. These measurements use the precision transmitters and receivers at large deep space antennas such as the ESTRACK stations (European Space Agency (ESA) TRACKing stations) at Perth and Madrid and the NASA DSN (Deep Space Network) antennas at Goldstone, Madrid, and Canberra (see Figure 55.4). The precision possible with these systems is impressive, with resolution of velocity changes of fractions of a millimeter per second and absolute locations in inertial space of a few centimeters now possible.

For the analysis of these radio science data and for theoretical simulations of planetary interiors with which to compare them, sophisticated numerical codes are used to compute accurate orbits of spacecraft from radio tracking data. Spatial and temporal variations in the gravity field can be used to determine physical properties of the interior and atmosphere of the planet. Since the beginning of the space age, the large-scale structure of the gravity field of planets and moons has been successfully used to determine the moment of inertia, which is a measure of the global density distribution and an important constraint on the interior structure.

FIGURE 55.4 Deep Space Network 70-m station at Goldstone, California.

In addition to global mass distribution, regional or local properties above target surface features can also be measured from the deviation of spacecraft trajectories. As an example, the Mars radio science experiment (MaRS) aboard Mars Express acquired gravity data during a number orbits above the Tharsis volcanoes, which form the largest volcanic region in the solar system.

The data analysis shows that the overall density of the volcanoes is higher than the average density of the Martian crust, in agreement with the basaltic composition of many Martian meteorites probably originating in the Tharsis area. One volcano, Ascraeus Mons, differs from the others in being of lower density in its upper part, although its overall density remains high. If the Tharsis Montes were built in succession by a single moving mantle plume, this suggests that Ascraeus Mons formed as the last of the Tharsis Montes. These data also show that Olympus Mons, the highest mountain in the solar system, lacks a low-density root, which indicates that it was built on a lithosphere of high rigidity, whereas the other volcanoes partly sank within a less rigid lithosphere.

Solid-body tides, which can be observed through their time-variable effect on the gravity field, can also provide information on the deep interior. These are particularly sensitive to global fluid layers such as a liquid iron core in terrestrial planets or an internal subsurface ocean in icy satellites. From the latest available data on the **moment of inertia** and the tidal amplitude of Mars, the best estimates yet obtained have been determined for the core size and composition of Mars. These show that the core size is expected to be between 1715 and 1850 km and that the weight fraction of sulfur in the core is between 13% and 18%. The addition of sulfur decreases the melting temperature of iron, and for the current estimates of the internal temperature of Mars, this high sulfur estimate implies that the core of Mars is entirely liquid and contains no solid inner part, in contrast to the Earth.

Constraints on planetary interiors can also be obtained from rotation variations. Three broad classes of rotation variations are usually considered: rotation rate (also called length-of-day) variations, orientation changes of the rotational axis with respect to inertial space (**precession** and **nutation**), and orientation changes of the planet's surface with respect to the rotation axis (polar motion and polar wander). These are due to both internal (angular momentum exchanges between solid and liquid layers) and external (gravitational torques) causes. As the rotational response depends on the planet's structure and composition, insight into the planetary interior can also be obtained. This is particularly so for the rotational variations due to well-determined external gravitational causes, such as for the nutations of Mars and the **librations** of Mercury and natural satellites.

Observation of the rotation may be performed using orbital measurements or, more precisely, by direct tracking

of landers on the surface of a planet. The latter will be the case with Rotation and Interior Structure Experiment (RISE) onboard the InSight Lander. Precise Doppler tracking from the Earth of a location on the Martian surface over extended periods (months to years) can be used to obtain Mars' rotation behavior. More specifically, measuring the relative position of the lander on the surface of Mars with respect to the terrestrial ground stations allows the reconstruction of Mars' time-varying orientation and rotation in space. Precession (long-term changes in the rotational orientation occurring over many tens of thousands of years) and nutations (periodic changes in the rotational orientation occurring on subannual timescales) as well as polar motion (motion of the planet's surface with respect to its rotation axis) are determined from this experiment and are used to obtain information about Mars' interior. Precession measurements improve the determination of the moment of inertia of the whole planet, which is particularly sensitive to the radius of the core. Using geochemical constraints to specify a plausible range of possible compositions, the core radius is expected to be determined with a precision of a few tens of kilometers (compared to $\sim$150 km currently). A precise measurement of variations in the orientation of Mars' spin axis also enables an independent (and more precise) determination of the size of the core via the core resonance in the nutation amplitudes. The amplification of this resonance depends on the size, moment of inertia, and flattening of the core. For a large core, the amplification can be very large, ensuring the detection of the free core nutation and determination of the core moment of inertia.

At the same time, measurement of variations in Mars' rotation rate reveals variations of the angular momentum due to seasonal mass transfer between the atmosphere and polar caps and zonal winds.

Investigation of the dependence of rotation variations, gravity field, and tidal variations on interior and atmosphere properties and orbital motion characteristics is essential to understand the interior and evolution of terrestrial planets. These studies include the development of advanced models of rotation, the construction of detailed models for the structure and dynamics of solid and fluid layers of the planets, the investigation of the dynamical response of these models to both internal and external forcing, the modeling of the orbital motion of large bodies of our solar system, and the inclusion of general relativistic effects into the data analysis.

4. INVESTIGATING PLANETARY INTERIORS USING HEAT FLOW MEASUREMENTS

The amount of heat escaping from a planet's interior is diagnostic of the subsurface temperature structure, which in turn is connected to the activity we observe on the surface. Essentially all geologic activity, except for meteorite impacts and wind and water erosion (which are powered by the sun), are driven by the internal heat engine of a planet. In addition, many material parameters of crustal and mantle rocks are temperature dependent, and subsurface temperatures influence the velocity of seismic waves, the **rheology** of crustal and mantle rocks, as well as the capability of crustal rocks to record **remanent magnetic fields** through the magnetic minerals' **Curie temperatures**. In addition, subsurface temperatures drive hydrothermal circulation in the crust, and, apart from pressure, temperature is the main factor controlling melting in the crust and upper mantle. Temperature differences also drive solid-state convection in the mantle and determine tectonic surface deformation to a considerable degree.

Heat emanating from a planetary interior derives in unknown proportions from primordial heat accumulated during accretion and core formation, and heat released by the decay of radioactive elements. Apart from the short-lived isotopes ^{26}Al and ^{60}Fe that have considerable influence on the earliest evolution of a planetary body, decay of ^{40}K, ^{232}Th, ^{235}U, and ^{238}U is the main source of heat in planetary interiors. Heat is transported to the surface through mantle convection and thermal diffusion, before it is finally radiated to space. Therefore, planets act like heat engines, and planetary cooling from initial temperatures after accretion and core formation is governed by the efficiency of the different heat transport mechanisms.

In order to quantify the heat flow from the Earth's interior, the first terrestrial heat flow measurements were conducted in the late 1930s by Bullard and Benfield, and tens of thousands of measurements have been performed since. It was found that heat flow varies substantially with tectonic setting, composition, and the age of rocks, and the average amount of heat lost from the Earth's interior was estimated to be of the order of 40 TW. It is estimated that only about 35% of the Earth's heat loss is balanced by present-day heat generation in the deep interior, while the bulk of the radiated energy is drawn from primordial heat accumulated during accretion and differentiation and previous radioactive decay. This implies that the Earth's interior is cooling more efficiently than a purely conductive sphere, a process likely driven by the plate tectonics cycle and the associated transport of hot mantle material to the surface at midocean ridges. However, the fraction of the heat released in the interior to that which is radiated to space, known as the Urey ratio, could have been significantly larger in the past due to greater radiogenic heat production and possibly less efficient cooling in previous epochs of the Earth's evolution.

4.1. Measurement Techniques

A measurement of the planetary heat flow requires knowledge of the subsurface temperature gradient as well

as the thermal conductivity of the material in which the measurement is made. The amount of heat passing perpendicularly through a surface of unit area is then given by Fourier's Law, $F = k\,\mathrm{d}T/\mathrm{d}z$, where k is the thermal conductivity (in units of W/m/K), $\mathrm{d}T/\mathrm{d}z$ is the thermal gradient (in units of K/m), and F is heat flow, or, more precisely, the heat flux density, in units of $\mathrm{W/m^2}$.

Apart from the heat originating in the planetary interior, temperatures at shallow crustal depths can be significantly affected by **diurnal**, annual, or even climatic changes of the surface temperature. While daily temperature fluctuations penetrate crustal rocks to depths of only a few meters, annual temperature variations have noticeable effects down to a few tens of meters, while glaciation cycles, which act on 100,000-year timescales, can affect subsurface temperatures to depths of a few kilometers. In order to measure the planetary heat flow, measurements must be conducted below the influence of these perturbations, or, alternatively, their influence must be taken into account by modeling.

Therefore, heat flow measurements on the Earth's continents are generally performed in boreholes whose depths extend from a few tens to a few hundreds of meters. The thermal gradient in the boreholes is determined by logging temperatures for extended periods of time, and the thermal conductivity of the host rock is generally determined from drill cores which are investigated in the laboratory. In contrast, because of its extremely stable surface temperature, measurements in the oceanic crust can be performed at much shallower depth, and probes derived from the original design by Bullard (see Figure 55.5) and having lengths of several meters are usually employed. This reduction in measurement depth is made possible by the almost isothermal conditions at the bottom of the oceans. In ocean bottom measurements, thermal conductivity of the sediments is usually determined from drill cores using needle probes in the laboratory, but can also be estimated from the cooling curves of the probes in situ. Integrated gradient and thermal conductivity probes using active heating techniques to determine thermal conductivity in situ were proposed by Christoffel and Calhaem in the late 1960s, and have been widely applied since then.

First attempts to measure extraterrestrial heat flows were made using ground-based radio observations in the early 1960s, but reliable results were only later obtained during the Apollo missions, where Bullard-like probes were emplaced in the lunar subsurface by the Apollo astronauts. Remote sensing techniques have also been proposed for extraterrestrial heat flow measurements, and microwave emissions, which are sensitive to temperatures at different depths for different wavelengths, could in principle be used to determine the thermal gradient in the lunar subsurface. Lacking insolation, surface temperatures in permanently shadowed polar craters are strongly influenced by interior heat flow, and infrared emissions from such regions could be used to estimate heat flow near the lunar poles from orbital measurements. However, there are large uncertainties associated with the interpretation of such data, so in situ measurements using borehole logging techniques remain the most reliable for surface heat flow determination to date.

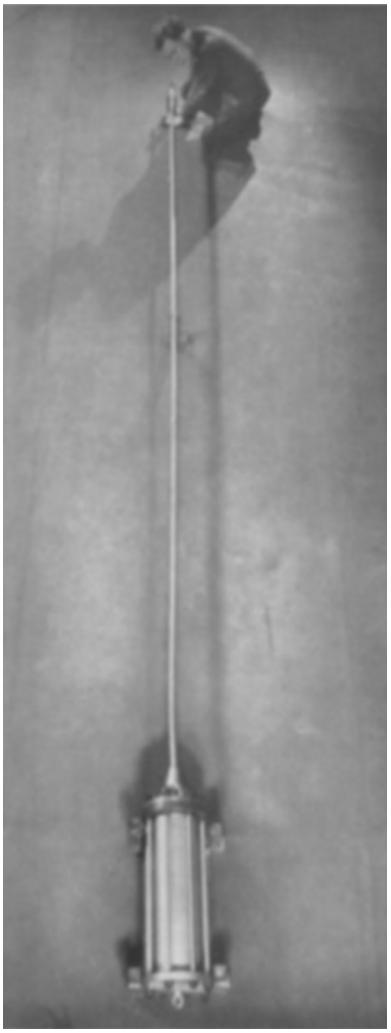

FIGURE 55.5 Original design of a heat flow probe for marine measurements by *Bullard (1954)*. The approximately 5-m-long and 3-cm-thick probe is equipped with temperature sensors to record the thermal gradient as well as the cooling of the probe after insertion into the sediments. Data logging equipment is located in the pressure-proof cylinder at the top of the probe (bottom of the image). *From Bullard (1954)*.

4.2. The Heat Flow of the Earth

The heat flow from the Earth's interior has been determined at more than 20,000 field sites in both continental and oceanic terrains, and a representation of the data is shown in Figure 55.6. Surface heat flow is largest near divergent plate boundaries where hot mantle material is advected

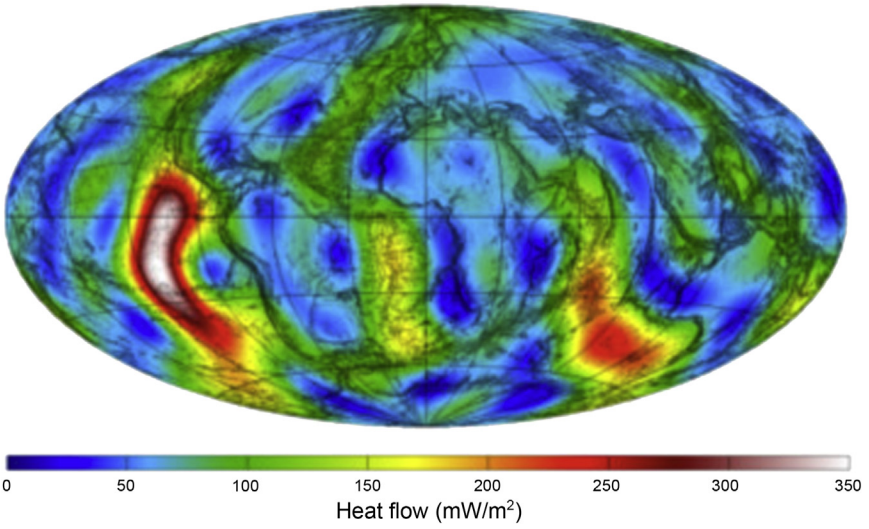

FIGURE 55.6 Color-coded map of the terrestrial heat flow derived from 24,774 measurements at 20,201 sites (*Pollack et al. (1993)*), plotted over a shaded relief topographic map (Hammer projection). Heat flow is at a maximum at midocean ridges where hot mantle material is advected toward the surface by mantle convection. Minimum heat flow is observed on the continental shields.

toward the surface, and heat flow in the oceanic lithosphere averages 101 mW/m^2. In contrast, continental heat flow is significantly less and measures only 65 mW/m^2 on an average. This difference is a direct consequence of the difference in heat transport efficiency, which is partly advective in the oceanic crust, but purely conductive in the continents. Heat flow on the continents is dominated by the heat released through radioactive decay in the crustal rocks, and is at a minimum in old continental regions. Taken together, the average heat loss from the surface of the Earth is 87 mW/m^2, corresponding to a total heat loss of 44.2 TW. Using numerical simulations, it has been shown that this heat loss corresponds to a present-day cooling rate of the Earth's mantle of 50 ± 25 K/Gyr.

The heat flow pattern observed on the Earth's surface reflects the action of the plate tectonics cycle, and surface heat flow is thus indicative of interior processes. Plate tectonics (see Evolution of Planetary Interiors and Earth: Surface and Interior) appear to be absent on planets other than the Earth, which is usually attributed to the lack of surface water on these bodies. Water acts to weaken the crustal rocks and facilitates breakup and finally subduction of the lithospheric plates.

The identification of large-scale heat flow variations on planets other than the Earth would further our understanding of heat transport mechanisms in these bodies, ultimately shedding light on the question why plate tectonics as observed on the Earth is unique in the solar system. Through analysis of the global heat flow data set it was found that the surface heat flow field correlates well with the seismic shear wave velocity in the upper mantle, thus establishing a link between seismic and heat flow investigations. For the Earth, heat flow data is collected and archived by the International Heat Flow Commission, and the global data set can be accessed through their website.

4.3. Lunar Heat Flow

In contrast to the Earth, structures like subduction zones, back-arc volcanoes, or midocean ridges are absent on the Moon, indicating the absence of plate tectonics. Instead, the Moon's interior can be viewed as an immobile outer shell underlain by a convecting mantle, a style of convection termed "stagnant lid convection". In fact, there is debate as to whether the Moon continues to convect. In any case, since no hot material is being transported directly to the surface, the heat flow pattern on the Moon only weakly reflects any mantle convection pattern, thus making the lunar surface similar to Earth's continental shields from a heat flow perspective.

Therefore, lunar heat flow mainly reflects the distribution and abundance of heat-producing elements in the lunar crust. Surface abundances of radioactive elements can be determined from orbit using gamma-ray spectroscopy, as gamma-ray data are sensitive to elements in the upper few decimeters of the crustal material. In this way, the Lunar Prospector mission between 1998 and 1999 determined elemental abundances on the lunar surface. It was found that K and Th vary widely across the surface, being significantly enriched in a region in the Oceanus Procellarum. This unique geochemical province was subsequently termed the Procellarum KREEP (for potassium (K), rare earth elements (REE), and phosphorus (P)) Terrane (PKT). A map of thorium on the Moon is shown in Figure 55.7. Thorium in the PKT is enriched by a factor of up to 10 with respect to the surrounding highlands, and although slightly elevated Th concentrations are observed

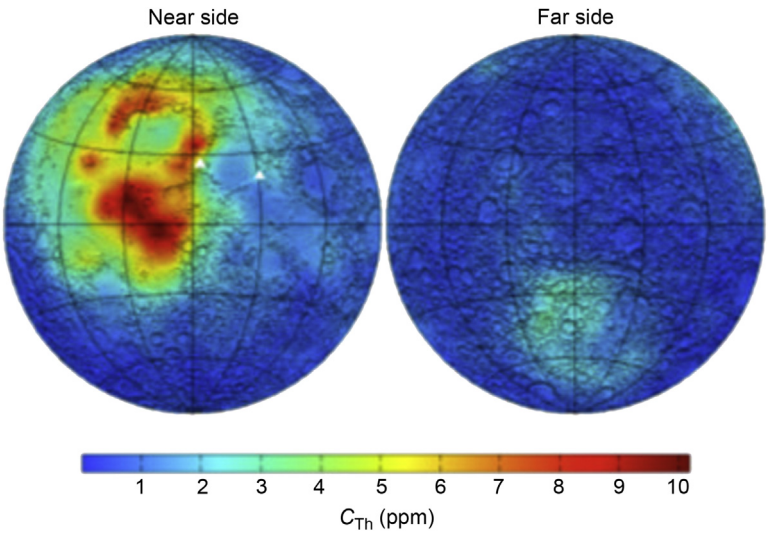

FIGURE 55.7 Surface abundance of Th as determined from Lunar Prospector gamma-ray data. The Procellarum KREEP terrane exhibits Th abundances which are elevated by up to a factor of 10 with respect to the lunar highlands. The Apollo 15 and 17 landing sites are indicated by triangles.

in the South Pole—Aitken Basin on the lunar farside, such large concentrations are absent anywhere else on the surface. However, from remote sensing data alone, the depth extent of the deposits cannot be determined, and in situ heat flow experiments are necessary to address this question.

While deep boreholes are needed to reliably determine the heat flow from the interior of the Earth, drilling deep holes on extraterrestrial bodies is inhibited by the mass of the necessary equipment. For the foreseeable future, the subsurface of the Moon will only be directly accessible to a depth of a few meters, and the deepest holes drilled by the Apollo astronauts extended to 2.4 m depth (Figure 55.8). Given that surface temperature fluctuations on the Moon are large, deeper boreholes might seem to be required for heat flow measurements. But the shallow depth of the boreholes is compensated by the low thermal conductivity of the lunar regolith, which rapidly attenuates surface temperature fluctuations. Thus nearly isothermal conditions are attained at a depth of only about 1 m, and temperature gradients can be reliably determined from data collected at shallow depth. Similar approaches would be feasible on Mercury or Mars. The latter environment is more challenging due to the presence of the Martian atmosphere, which acts to increase thermal conductivity and thus the penetration depth of temperature perturbations.

The history of extraterrestrial heat flow measurements starts with the ill-fated Apollo 13 mission, and the first successful measurement was not performed until Apollo 15. Technical problems during the emplacement of the probes on Apollo 16 frustrated a successful measurement during that mission, and only one further successful measurement was performed during Apollo 17 before the Apollo program ended. Material including images, videos, and radio communication transcriptions connected to the Apollo missions is accessible through the Apollo Lunar Surface Journal Web sites maintained by NASA.

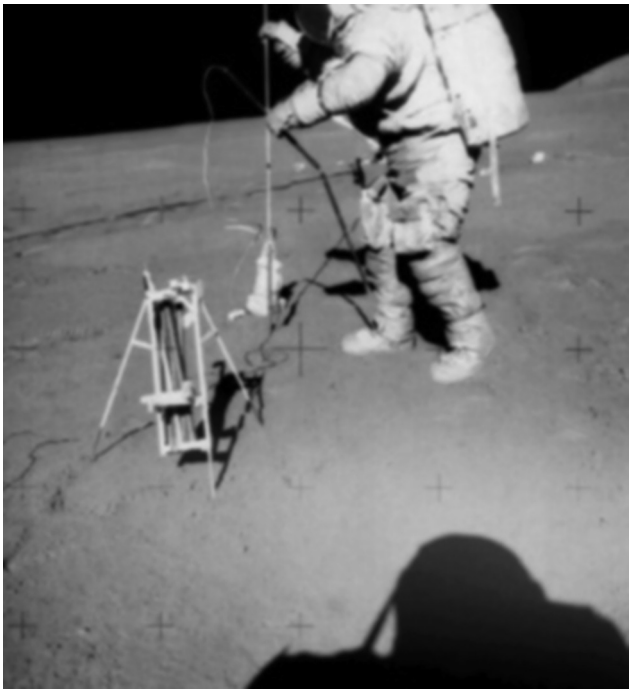

FIGURE 55.8 The heat flow experiment during emplacement on Apollo 15. The drill rack is in the foreground and the Apollo lunar surface drill is on the surface behind the borestem, which is emplaced in the ground. The dark, two-segment rod in the left hand of the crewman is the heat probe. The white probe emplacement tool is in his right hand (*Apollo image AS-15-92-12407*).

For Apollo 15, thermal gradients were determined to depths of up to 1.4 m, while the Apollo 17 probes were emplaced to a final depth of 2.4 m (Figure 55.9). Thermal

FIGURE 55.9 The Apollo 17 heat flow probe after emplacement in the borehole. The probe is connected to the Apollo Lunar Surface Experiment Package central station in the background. *Apollo image AS17-134–20496.*

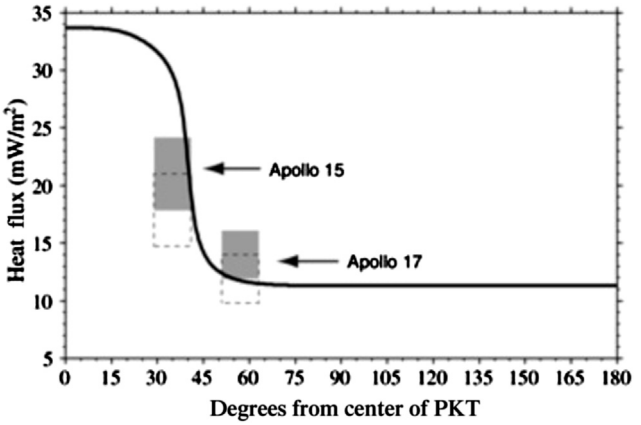

FIGURE 55.10 Modeled present-day lunar heat flow as a function of distance from the center of the Procellarum KREEP terrane (PKT). Initial heat flow estimates derived for the Apollo 15 and 17 measurements are indicated in gray, and subsequent corrections accounting for lateral heat transport in the lunar crust are shown as dashed rectangles. The sizes of the rectangles indicate the measurement uncertainty. *Figure from Wieczorek & Phillips (2000).*

conductivity was determined in situ from a line heat source method, and thermal diffusivity κ was independently estimated from the attenuation of the annual temperature wave. Together with measurements of density ρ and heat capacity c_p on drill core samples returned to the Earth, thermal conductivity $k = \kappa/\rho c_p$ could be independently estimated from the thermal diffusivity measurement. Results of the latter method were finally given preference over the line heat source data, as it was concluded that the direct heating method likely overestimated thermal conductivity due to regolith compaction during probe emplacement.

From these measurements, Langseth and colleagues estimated heat flows of 21 and 16 mW/m^2 at the Apollo 15 and 17 sites, respectively, and the average lunar heat flow was estimated to be 18 mW/m^2. Accounting for effects of lateral heat transport, these values were later revised downward and an average heat flow of 12 mW/m^2 was determined. This heat flow corresponds to a bulk lunar Uranium concentration of 20 ppb, a value close to that derived for the silicate fraction of the Earth, lending support to the hypothesis that the Moon reaccreted from the debris after a giant impact of a Mars-sized planetary body with the proto-Earth. However, it should be kept in mind that the wealth of new data returned by recent lunar missions (SELENE, Gravity Recovery and Interior Laboratory (GRAIL)) suggests that the average crustal thickness is less than previously thought and that it maintains significant porosity to depths of tens of kilometers. Therefore, a fresh look at the implications of the Apollo measurements is warranted.

Models of the heat production in the lunar interior indicate that the observed concentration of heat-producing elements in the Procellarum region must be the surface expression of a larger reservoir at depth. The Apollo heat flow data are compatible with the local presence of a KREEP layer up to 10 km thick at the base of the lunar crust (see Figure 55.10), which would be in line with the persistent volcanic activity observed in the region. Youngest mare basalts are only slightly over 1 Gyr old, and it has been speculated that the concentration of heat-producing elements in the PKT could have been caused by large-scale mantle flow following the gravitational overturn of a freezing magma ocean that likely covered the Moon following accretion. However, further heat flow measurements would be needed to corroborate this view and, ideally, future measurements should be conducted in the center of the PKT and/or far away in the lunar highlands. The latter would be unaffected by the surface concentrations of heat-producing elements and be more representative of the global average.

4.4. Future Investigations

Future lunar heat flow measurements are currently being studied in the frame of an international collaboration termed the International Lunar Network, but definite plans for mission implementation do not exist at present. However, the recently selected Discovery-class mission InSight, which is due to launch in 2016, will place a geophysical lander carrying a heat flow probe in the southern Elysium region of Mars in September 2016. The heat flow probe,

termed the Heat flow and Physical Properties Package, or HP^3 for short, is built to access the Martian regolith to a depth of up to 5 m by means of a hammering mechanism, emplacing a suite of temperature sensors into the subsurface. The overall measurement approach is similar to that taken by Bullard or Langseth, and a depth-resolved measurement of the subsurface temperatures will be used to determine the thermal gradient. Active heating elements inside HP^3 will be used to determine the thermal conductivity in situ, and the attenuation of the annual temperature wave will be used to independently estimate thermal diffusivity and to provide a consistency check for the thermal conductivity value determined from active heating.

While a single heat flow measurement is hardly enough to confidently constrain the average heat flow from a planet, the InSight measurement will provide an important baseline. In addition, the seismic experiment on InSight will provide an estimate of crustal thickness, which can be used to validate thickness models derived from gravity data. The thickness of the crust is a key constraint needed to interpret local heat flow measurements in terms of the global average. Furthermore, the heat flow pattern on the Martian surface is expected to be much simpler than that of either the Earth or the Moon for two reasons: First, Mars currently lacks a plate tectonics cycle (although it may have possessed one during its earliest evolution), and second, Mars does not show any geochemically anomalous regions like the PKT of the Moon (compare Figure 55.11). Therefore, a first global estimate of the average heat flow can be derived from the InSight data, but further measurements in different locations are clearly desirable.

Another device built to measure the energy balance at the surface of an extraterrestrial body is the Rosetta MUPUS instrument (MUlti PUrpose sensor for Subsurface observation), currently on its way to comet 67p/Churyumov–Gerasimenko. Its goal is to measure the heat flow into the comet, the largest unknown contribution to the surface energy balance of the comet. The instrument will be delivered to the cometary surface onboard the Rosetta Philae Lander and is shown in Figure 55.12. MUPUS consists of a 35-cm-long rod equipped with temperature sensors and heaters, and a hammering mechanism is mounted on top of the rod to emplace it into the ground. The instrument will then determine the surface temperature, subsurface thermal gradient, as well as the thermophysical properties of the cometary regolith, thus quantifying the heat flow into the comet and help to detail the solar energy input responsible for driving activity and liberating gas and dust to the cometary coma and tail.

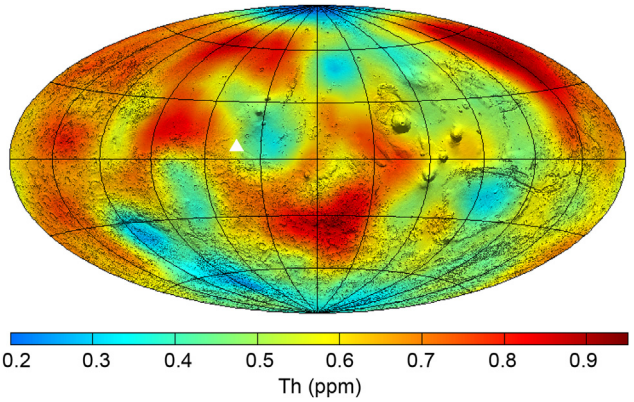

FIGURE 55.11 Abundance of Th on the Martian surface as determined from gamma-ray spectroscopic measurements of the Mars Odyssey spacecraft.

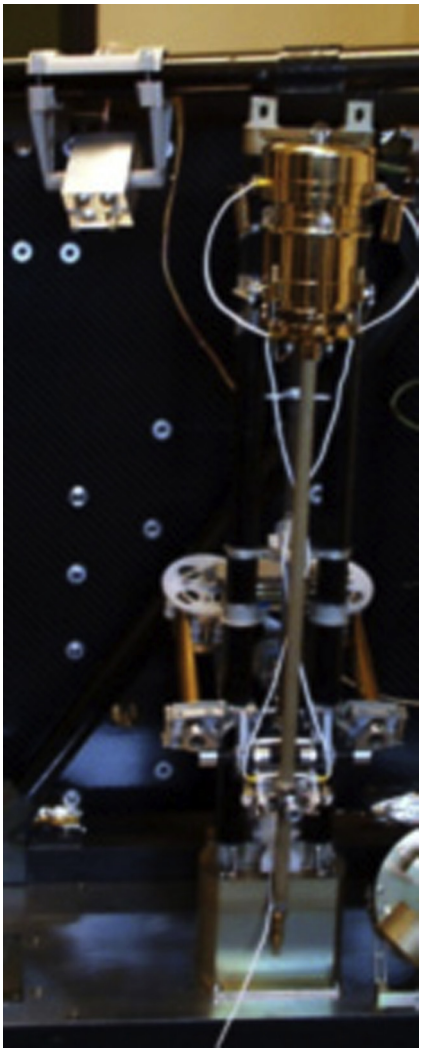

FIGURE 55.12 The Multi Purpose Sensor (MUPUS) onboard the Rosetta Lander Philae, currently on its way to rendezvous the comet 67p/Churyumov–Gerasimenko in 2014. The MUPUS probe on the right-hand side of the picture houses 16 temperature sensors, which can simultaneously be operated as heaters for thermal conductivity determination. MUPUS will be deployed away from the lander using an extendable boom. The golden cap houses a hammering mechanism which will drive the probe into the cometary surface. *From Spohn et al. (2007).*

Other measurement approaches which have been proposed to determine heat flow on extraterrestrial bodies include the so-called flux plates, which can measure surface heat flow in environments with constant surface temperatures. Flux plates are placed on the planetary surface from which the heat flow is to be measured, and the temperature difference across a layer of known thermal conductivity is recorded. Such a device would be suited to determine the heat flow on Venus, whose rocky surface precludes drilling to any significant depth. The constant cloud cover and very dense atmosphere of Venus result in very stable surface temperatures, such that a flux plate measurement could be successfully executed there. Such a measurement would provide a very important constraint on how Earth-sized planets without plate tectonics lose their heat. Many models of the interior evolution of Venus speculate that it should currently be heating up, resulting in a present-day Urey ratio >1.

5. INVESTIGATING PLANETARY INTERIORS USING EM SOUNDING

EM sounding encompasses a wide variety of methods used to sense subsurface structure from depths of less than a few meters to a thousand kilometers or more. EM sounding is distinct from surface-penetrating radar (or its seismological cousins) in being inductive rather than wavelike: the diffusive transfer of energy is akin to that in heat flow, groundwater, and electrical circuits. This transition to induction occurs at low frequency, in the kilohertz to megahertz range depending on ground electrical conductivity. Thus a vast part of the EM spectrum, from below 1 μHz to perhaps 1 MHz, is within the realm of EM sounding. In this section we will be focusing on the so-called passive techniques—those that use natural EM energy in planetary magnetospheres, ionospheres, and atmospheres as the source.

Electrical conduction in the familiar sphere of Earth's upper crust is largely electrolytic, i.e. by movement of ions in water—conductivity increases with porosity and fluid content. In frozen H_2O systems, conduction through ice and hydrates is protonic, through charge defects resulting from lattice substitutions of salts, acids, and bases. Analogous substitutions by iron, aluminum, oxygen, and hydrogen in silicates result in electronic semiconduction, both from electrons and holes. Conductivity is also strongly temperature dependent. In contrast, the outer portions of all other silicate or icy bodies in the solar system are likely to be much more resistive than the Earth, for the simple reason that free water is lacking. This opens up these regions to EM sounding at higher frequencies (see below), which in turn provides better measurements and more convenient signal integration.

The effective penetration depth for EM waves is a strong function of frequency and resistivity. The EM skin depth (in meters) is given by $\delta = 500/\sigma^{1/2} f^{1/2}$, where σ is the conductivity (S/m) and f is the frequency (Hz). This relation indicates what frequencies are necessary to probe to a specified depth at a particular average conductivity. For example, terrestrial exploration geophysics seeking targets at several tens of meters to several kilometers depth utilizes frequencies from $\sim$10 mHz to 10 kHz, but mantle studies require 10 μHz or lower. Conversely, the lunar lower mantle has been adequately sounded in the millihertz range, but better characterization of the more resistive upper mantle and crust will require frequencies up to 1 Hz or higher.

In practice, the true conductivity vs depth is determined from the apparent conductivity (or other measurement parameters; see below) vs frequency using classical inverse methods. Note that unlike the potential field methods discussed above, EM inversions are not formally nonunique. The inversion can be thought of as assigning the conductivity at the highest measured frequency to the uppermost layer, and progressively solving for the conductivity at greater depths by comparing the apparent conductivity at the next depth to the true conductivity of the overlying material.

5.1. Natural Sources

Within the low-frequency branch of diffusive EM, the primary division of techniques is between those that use an artificial source (a transmitter) and those that rely on natural sources. The former enjoy considerable flexibility and high signal to noise but require significant additional resources and are generally limited to investigation depths of several kilometers. On Earth, abundant energy exists at less than 1 Hz from magnetospheric pulsations and the interaction of the magnetosphere with diurnal heating of the ionosphere. Above 1 Hz, the ground—ionosphere waveguide allows lightning energy to be recorded globally as the low-frequency Schumann resonances and regionally at higher frequencies. These signals are collectively known as spherics. These sources of energy for EM sounding will likely be present on other bodies with magnetospheres, ionospheres, and chargeable atmospheres. In interplanetary space, temporal variations in the plasma density of the solar wind provide signals that have already been exploited for lunar sounding. Finally, special circumstances around specific planets can provide unique sources; in particular, the inclination of satellite orbits with respect to the static magnetic field of Jupiter yields an apparent time variation at the orbital period. Overall, some kind of ambient energy is likely present at most bodies that would enable EM sounding.

TABLE 55.1 Approaches to Natural Source EM Sounding

Method	Measurements	Number of Stations	Comments
Transfer function (TF)	Magnetic field B	2	Determine source field by distant second station unaffected by target
Transfer function-1 (TF-1)	B	1	Special cases using prior knowledge of source field *or* target is "perfect" conductor
Geomagnetic depth sounding (GDS)	B	3 or more	Compute impedance from vertical field and horizontal gradients
Geomagnetic depth sounding (GDS-1)	B	1	Special case where horizontal gradient can be computed using known periods and length scales
Magnetotellurics (MT)	B + Electric field	1	General single-station method
Wave tilt (WT)	Electric field	1	General single-station method

5.2. Measurement Techniques

The fundamental quantity that must be derived in any sounding is the frequency-dependent EM impedance Z, and it is the variety of approaches to Z that lead to more individual techniques in EM than in any other geophysical method. A commonly used parameter, the apparent conductivity, is simply related to the impedance as $\sigma_a = \mu\omega/Z^2$, where μ is the permeability and ω is the angular frequency. Apparent conductivity is useful because it is dimensionally identical to true conductivity but instead represents an aggregate response of the target.

Two known quantities are necessary to determine the impedance (see Table 55.1). One of these quantities is nearly always the magnetic field B near the target, i.e. the sum of source and induced magnetic fields. Note that measurement need not be made at the surface, as long as it is at an altitude substantially less than one skin depth at the highest frequency of interest. This can include spacecraft if the desired exploration depth is sufficiently large. Active methods can measure either electric or magnetic fields; the second known quantity is the transmitted signal.

The magnetic transfer function (TF) method is straightforward, measuring three components of the magnetic field at a location on or near a planetary body and comparing that to a measurement distant from the body. This relates the sum of source and induced fields to the source field alone, from which the induced field and internal conductivity structure can be derived. The TF method was used for Apollo-era lunar soundings. In a few special cases (TF-1) of accurately characterized natural signals—the Earth's ring current or the time variation introduced by the motion of the Galilean satellites in Jupiter's main field—the source can be specified a priori, so a single platform is sufficient. Single-magnetometer characterization can also be performed where the target can be approximated as a perfect conductor, like the Moon's core.

Geomagnetic depth sounding (GDS) uses surface arrays of magnetometers to determine impedance from the ratio of vertical B to the magnitude of the horizontal gradient of B. Because the wavelength in the ground $\lambda = 2\pi\delta$, GDS requires array spacing comparable to the skin depth in order to resolve the relevant horizontal wave structure. This calls for dense arrays to resolve the outer tens to hundreds of kilometers of planetary bodies.

In the magnetotelluric (MT) method, measurement of the electric field E supplies the required second piece of information and enables complete EM soundings from a single station. Finally, the wave-tilt (WT) method is preferable for aerial surveys because the quadrature horizontal E (containing most of the inductive signal) can be readily determined by comparison to the vertical E.

Only magnetic methods have been used heretofore in planetary exploration because of their simplicity: electric field measurements are more challenging at low frequencies and noninductive contributions to E must be identified. Nonetheless, those methods using E have the significant advantage of complete soundings from a single vehicle that do not require a priori knowledge or special conditions.

5.3. Terrestrial Exploration

Regional EM soundings of the crust and upper mantle of the Earth began in the 1960s using magnetometer arrays (GDS) and have since been supplemented by MT. The deepest soundings in the mantle use very long period signals from reasonably well-known sources. Two examples here illustrate how EM sounding can elucidate regional

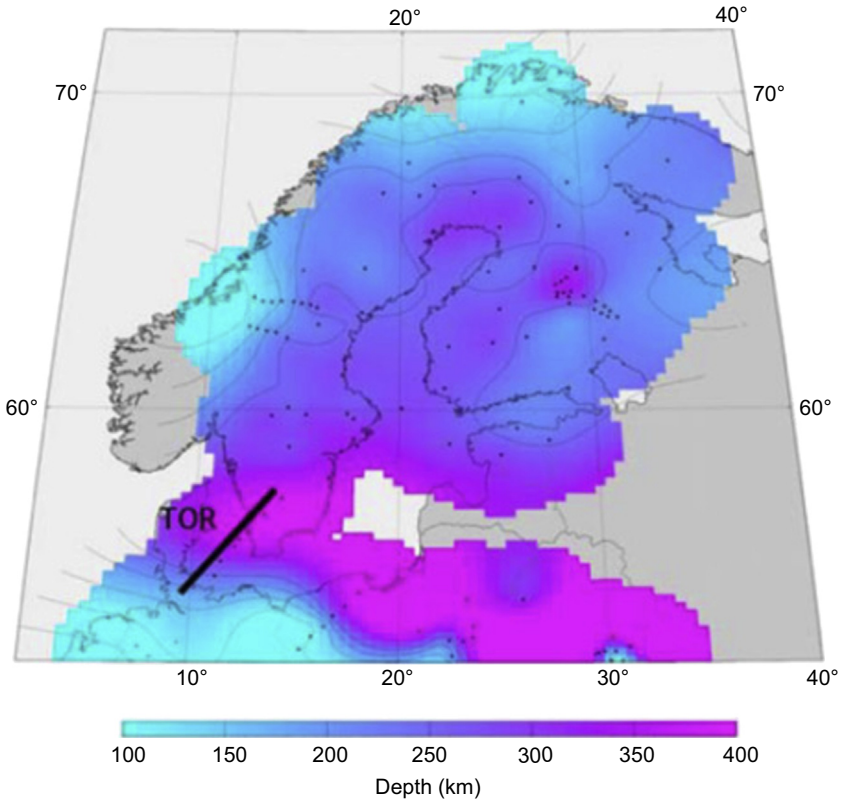

FIGURE 55.13 Thickness of the thermal lithosphere in northern Europe compiled from magnetotelluric soundings. Profile "TOR" crosses the Trans-European Suture Zone, a region of thickening caused by multiple plate tectonic collisions. *Korja (2007)*.

variations in upper mantle structure (Figure 55.13) or deep mantle structure (Figure 55.14). At present, fully three-dimensional images of the Earth are emerging, using decades of observations from hundreds of geomagnetic observatories.

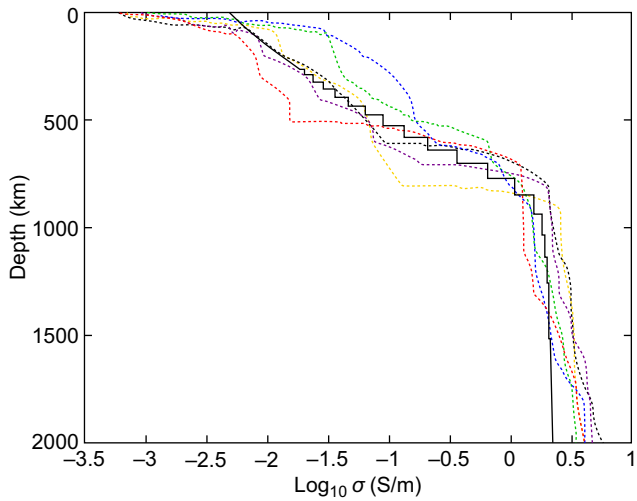

FIGURE 55.14 Electrical conductivities at six European stations (in various colors) and global average (black) from MT and GDS methods (*Semenov & Kuvshinov (2012)*). Much current work in interpreting these kinds of profiles using laboratory data focuses on the tradeoff of temperature (including partial melting) vs dopants such as trace amounts of water.

Variations in electrical conductivity revealed by EM sounding are interpreted in terms of temperature and composition. The former dominate Figure 55.13 where the thickness of cold lithosphere is doubled in the Trans-European Suture Zone. Both may affect the deep profiles of Figure 55.14. The effect of trace quantities of water (hundreds of ppm) in the Earth's mantle is hotly debated.

5.4. Magnetic Sounding of the Moon

During the Apollo Program, a variety of lunar surface experiments were performed in geophysics, space physics, and astrophysics. Simultaneously, the robotic Explorer program was reaching full stride. The Apollo 12 surface magnetometer performed continuous dayside measurements for several months; throughout this time the Explorer 35 spacecraft, also including a magnetometer, orbited the Moon at distances up to several thousand kilometers. The two instruments jointly recorded fluctuations in the Earth's magnetotail and the solar-wind-embedded interplanetary magnetic field from 10^{-5} to 3×10^{-2} Hz. EM sounding was performed using the frequency-dependent magnetic TFs. Due to the fact that the outer portions of the Moon are so electrically resistive (because it is both cold and dry), measured EM waves at even the highest observed frequency penetrate a few hundred kilometers before being able to induce measurable eddy

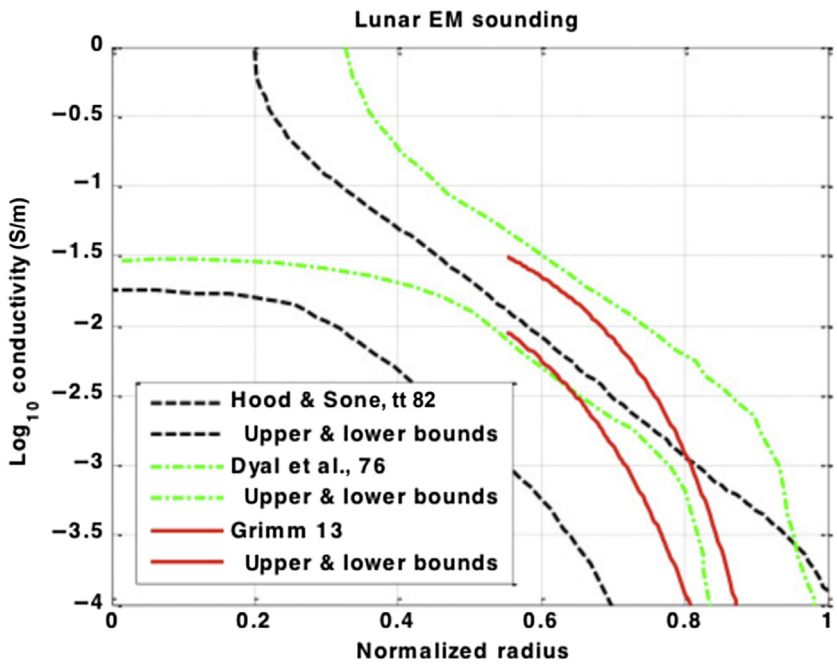

FIGURE 55.15 Electrical conductivity of the Moon, derived by comparing the time-varying magnetic field at the lunar surface with that of a distant satellite (transfer function method). Conductivity increases with depth due to increasing temperature. The large uncertainty at depth is because the volume fraction is so small. Results are also poorly constrained at depths less than a few hundred kilometers (normalized radius >0.8) because this region is so resistive it is transparent to the millihertz signals used for the soundings. Conductivities in the midmantle (normalized radius = 0.7, 500 km depth) indicate higher than expected temperatures (1600 K), perhaps due to higher radionuclide abundance or a thermally insulating megaregolith. Alternatively, impurities such as Fe^{3+}, Al^{3+}, or H^{+} can raise the mantle conductivity.

currents. Hence there are large uncertainties in the electrical properties of the lunar crust and upper mantle. Conversely, the lowest frequencies ($\ll 10^{-4}$ Hz) fully penetrate the Moon but are relatively insensitive to the innermost 20–30% of the radius (Figure 55.15).

Although the Apollo Explorer TFs established an upper limit to the size of a lunar core, better bounds were determined many years later during the Lunar Prospector mission. External magnetic field lines are nearly parallel when the Moon is passing through Earth's magnetotail. If the permeability–conductivity product of the core is very large—effectively equivalent to infinite conductivity—the induced fields will completely exclude the source field, so the induced dipole produces a perturbation to the parallel external field lines that depends only on the core size (Figure 55.16). The resulting bounds 340 ± 90 km are consistent with seismology and laser ranging. It is also worth noting that magnetic **hysteresis** measured with Apollo Explorer indicates 4–14 wt% free iron, depending on assumptions of bulk mineralogy.

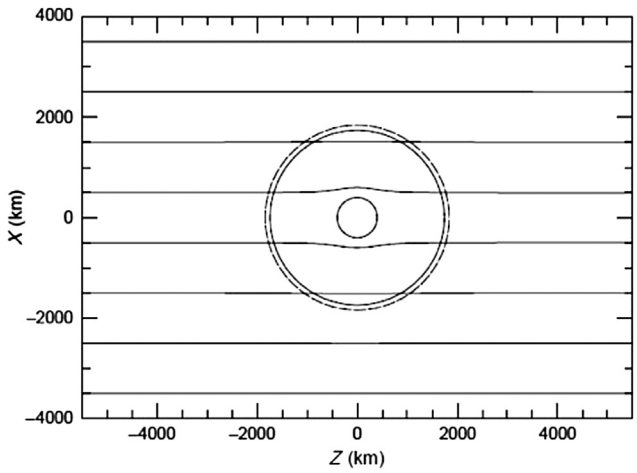

FIGURE 55.16 Modeled deflection of field lines in the Earth's magnetotail by a perfectly conducting lunar core of radius 400 km (inner circle). This is a feature of time-varying signals: eddy currents in the conducting core exclude the primary magnetic field, whereas a static field would be focused into a magnetically permeable core. A range of core radii 250–430 km was found to match small perturbations observed by the Lunar Prospector spacecraft at the outermost circle. *Hood et al. (1999)*.

5.5. Magnetic Sounding of the Galilean Satellites

Among the most significant results of the Galileo mission was the discovery of EM induction signatures in the magnetometer records for flybys of Io, Europa, and Callisto, and perhaps for Ganymede as well. Because the conductivity of solid ice or rock is small, salty subsurface oceans on the icy satellites and a global partial melt layer on Io are the most likely causes of these signatures. Jupiter's massive magnetic moment produces field amplitudes of 4–1700 nT at the Galilean satellites and because this field is not orthogonal to the plane of the satellites, it varies periodically with **synodic periods** of 10–13 h as viewed from the satellites. The result is a source field variation of $\sim 10^{-6}$ Hz with known amplitude and direction, so the TF can be evaluated using the Galileo spacecraft alone (TF-1). The depth to and conductivity of the

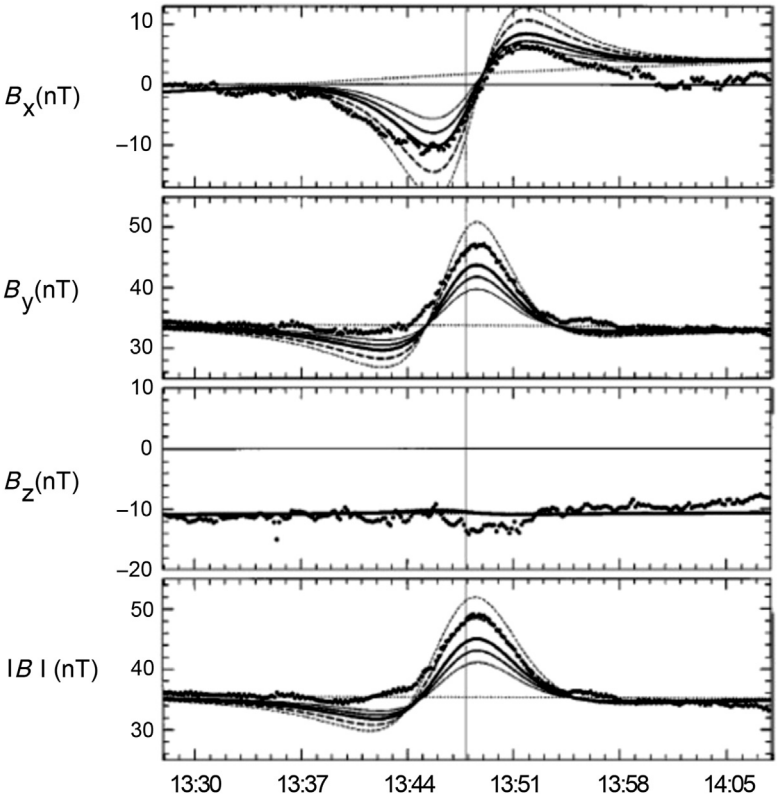

FIGURE 55.17 Galileo magnetometer data (dots) at Callisto flyby on June 25, 1997, compared to various induction models for internal oceans (lines). The temporal variation in Jupiter's static field due to its inclination with respect to Callisto's orbit causes inductive eddy currents to flow in the satellite's interior, forming an induced dipole. This dipole is evident in the raw data above and because its orientation always opposes the main field, it cannot have a static origin. *Zimmer et al. (2000)*.

internal water or magma oceans can be inferred to be tens of kilometers and ∼1 S/m, respectively. Skin effects allow these fields to penetrate through much of the satellite, but ocean thicknesses are harder to estimate because EM sounding is sensitive only to the conductance (the product of conductivity and thickness) when trying to assess a highly conductive layer. Nonetheless, magma and water ocean thicknesses of 100−200 km have been derived (Figures 55.17 and 55.18).

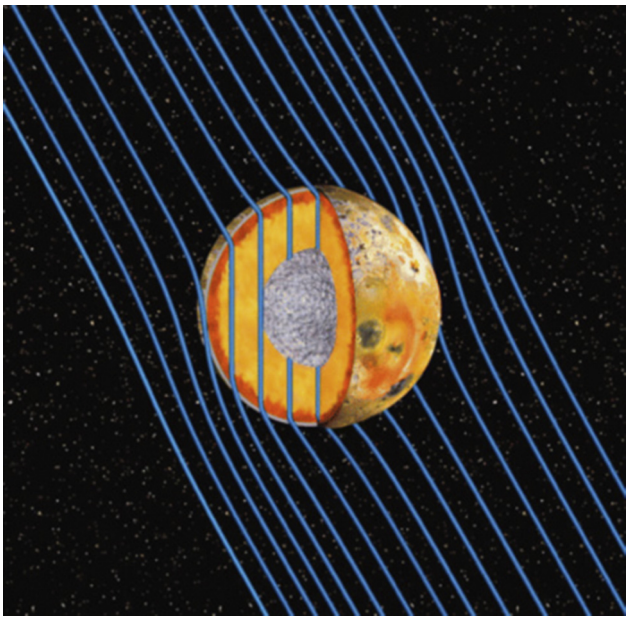

FIGURE 55.18 Internal structure of Io revealed by EM sounding (TF-1 method). Red layer ∼40 to >90 km deep is the global partial melt. *Khurana et al. (2011)*.

5.6. Future Exploration

Many missions can exploit EM sounding of planetary interiors using natural sources and simple sensor configurations. A significant magnetosphere makes Mercury the most Earth-like in terms of classical natural EM sources, yet frequent **reconnection** events define an even more dynamic environment. Its core will also be a prime EM target and the conductivity profile in the mantle may show whether it is convecting or whether the lithosphere comprises the entire mantle. The iron content of the mantle may also be recovered.

With a shielding ionosphere and no defined external sources, EM soundings of Venus must be performed from the surface or atmosphere, but both ionospheric disturbances and lightning are known to exist. A balloon in the benign middle atmosphere can perform long-duration remote sensing of the subsurface using MT or WT. The dearth of water on Venus implies that these signals will penetrate tens of kilometers into the ground enabling the mean thickness and lateral variations of the **thermal lithosphere** to be determined.

FIGURE 55.19 Concept for a lunar geophysical station including a magnetotelluric sounder. Three spring-launched orthogonal wires have electric field sensors at their tips, whereas boom at left supports fluxgate and search-coil magnetometers. Other instruments include seismometer, heat flow probes (2), and retroreflector. *Courtesy Jet Propulsion Laboratory.*

EM soundings of the Moon can be improved by expanding the frequency range: shallower skin depths at higher frequencies can resolve the outer resistive portions, and stable long-term measurements may detect the core and distinguish molten silicate from iron. Low-altitude orbital coverage or a surface network (Figure 55.19) would allow geographic variations to be resolved, for example, if the Moon's most volcanically active regions are also distinct in the upper mantle.

The cold surface and lower heat flow of Mars result in a cryosphere many kilometers thick, putting liquid groundwater and potential stable microbial habitats out of reach of conventional planetary remote or in situ sensing. This conductivity contrast would be comparable to that observed for the Galilean satellites, and its depth would provide a ready estimate of geothermal gradient.

The extremely low frequency time variations developed at the satellites of Jupiter by their inclined orbits with respect to the main field will also be present at Uranus and Neptune. This will enable single-magnetometer global TF soundings for close flybys of satellites of the ice giants. Saturn's satellites have negligible inclination with respect to the main field, but for all the giant planets, the diversity of magnetospheric phenomena may provide a rich spectrum of EM signals. Titan is of course different because of its atmosphere; like Venus, MT or WT measurements from landed or aerial assets could exploit ionospheric disturbances or lightning.

6. SUMMARY

For the past 40 years, the geophysical exploration of the deep interiors of the terrestrial planets had lagged far behind the exploration of their surfaces. This is partly due to the difficultly in making the necessary precise measurements, which often requires multiple long-lived surface platforms for the best results, and partly due to the difficultly in generating the same level of public excitement as a surface mission, with its easily communicated imagery and sense of exploration. However, the scientific value of these measurements is unquestioned, and we now stand at the beginning of a new era of geophysical missions. The GRAIL mission has recently completed its mapping of the gravity field of the Moon at unprecedented resolution, and MESSENGER (MErcury, Surface, Space ENvironment, GEochemistry and Ranging) is currently exploring the interior of Mercury with gravity and magnetic measurements from orbit. Also, the InSight mission to Mars will, starting in late 2016, obtain surface seismic, heat flow, and magnetic measurements which will allow us to address many of the fundamental questions regarding the structure, origin, and evolution of Mars. Looking farther ahead, ESA is studying INSPIRE (Integrated Network of Seismic Probes to Invigorate Robotic Exploration), a Mars geophysical network mission to use multiple landers to sharpen the seismic resolution of that planet's interior, and there are plans within NASA to explore the possibility of a habitat/environment on Europa using geophysical techniques to probe the extent of its putative subcrustal ocean. Thus the next decade promises to be an exciting one for planetary interior exploration.

BIBLIOGRAPHY

Bullard, E. (1954). The flow of heat through the floor of the Atlantic Ocean. *Proc. Roy. Soc. London A, 222*, 408–429.

Grimm, R. (2002). Low-frequency electromagnetic exploration for groundwater on Mars. *Journal of Geophysical Research, 107*, 1–29.

Hood, L., et al. (1999). Initial measurements of the lunar induced magnetic dipole moment using Lunar Prospector Magnetometer data. *Geophysical Research Letters, 26*, 2327–2730.

Jaupart, C., & Mareschal, J.-C. (2007). *Heat flow and thermal structure of the lithosphere*. In G. Schubert (Ed.), *Treatise on geophysics* (Vol. 10); (pp. 217–252). Oxford: Elsevier Ltd.

Khurana, K., et al. (2011). Evidence of a Global Magma Ocean in Io's Interior. *Science, 332*, 1186.

Korja, T. (2007). How is the European lithosphere imaged by magnetotellurics. *Surveys in Geophysics, 28*, 239–272.

Lognonné, P., & Johnson, C. (2007). *Planetary seismology*. In G. Schubert (Ed.), *Treatise on geophysics* (Vol. 10); (pp. 69–122). Oxford: Elsevier Ltd.

Pollack, H. N., et al. (1993). Heat flow from the Earth's interior: Analysis of the global data set. *Reviews of Geophysics, 31*(3), 267–280.

Semenov, A., & Kuvshinov, A. (2012). Global 3-D imaging of mantle electrical conductivity based on inversion of observatory C-responses - II. Data analysis and results. *Geophysical Journal International, 191*, 965–992.

Spohn, T., Seiferlin, K., Hagermann, A., Kollenberg, J., Ball, A. J., Banaszkiewicz, M., et al. (2007). MUPUS – a thermal and

mechanical properties probe for the Rosetta Lander Philae. *Space Science Reviews, 128*, 339–362.

Wieczorek, M. (2007). *The gravity and topography of the terrestrial planets*. In G. Schubert (Ed.), *Treatise on geophysics* (Vol. 10); (pp. 165–206). Oxford: Elsevier Ltd.

Wieczorek, & Phillips. (2000). The Procellarum KREEP Terrane: Implications for mare volcanism and lunar evolution. *Journal of Geophysical Research, 105*, 20417–20430.

Zimmer, C., et al. (2000). Subsurface oceans on Europa and Callisto: Constraints from Galileo magnetometer observations. *Icarus, 147*, 329–347.